Importance of Madelung Potential in Quantum Chemical Modeling of Ionic Surfaces

GIANFRANCO PACCHIONI,[1]* ANNA MARIA FERRARI,[1] ANTONIO M. MÁRQUEZ,[2] and FRANCESC ILLAS[3]

[1]Dipartimento di Chimica Inorganica, Metallorganica e Analitica, Università di Milano, via Venezian 21, 20133 Milano, Italy; [2]Departamento de Quimica Fisica, Facultad de Quimica, Universidad de Sevilla, 41012 Sevilla, Spain; and [3]Departament de Quimica Fisica, Universitat de Barcelona, C/Marti i Franques 1, 08028 Barcelona, Spain

Received 21 January 1996; accepted 13 July 1996

ABSTRACT

The importance of the inclusion of the Madelung potential in cluster models of ionic surfaces is the subject of this work. We have determined Hartree–Fock all electron wave functions for a series of MgO clusters with and without a large array of surrounding point charges (PC) chosen to reproduce the Madelung potential. The phenomena investigated include: the reactivity of surface oxygens toward CO_2, atomic hydrogen, and H^+; the geometry and adsorption energy of water and the vibrational shift of CO adsorbed at Mg^{2+} sites; the electronic structure and the hyperfine coupling constants of oxygen vacancies, the paramagnetic F_s^+ centers. While some clusters give results which are virtually independent of the presence of the PCs, other clusters, typically of small size, give physically incorrect results when the PCs are not included. The embedding of the cluster in PCs guarantees a similar response for clusters of different size, at variance with the bare clusters, where the long range coulombic interactions are not included.

Introduction

In the past 5 years, a large and constantly increasing number of quantum chemical studies of ionic materials and, in particular of ionic oxides, has been reported.[1–46] The reason is the considerable interest in the theoretical description and in the computer simulation of the electronic properties of oxides and of their chemical behavior which is relevant in chemistry, solid state physics, and material science. Most of these studies have been performed using the cluster model approach[4] in which the infinite oxide crystal is represented by just a few atoms (or ions).[5–38] This is the same approach largely employed to study adsorption on

* Author to whom all correspondence should be addressed.

CCC 0192-8651 / 97 / 050617-12

metals, and is alternative to the more rigorous, but computationally less flexible, band structure approach in which the periodic nature of the surface is explicitly taken into account.[39–49] Usually, cluster models of oxide surfaces consist of a small number of ions surrounded by a large array of point charges, PCs, determined in such a way to reproduce the Madelung potential in the chemisorption region.[5–29] The Ewald technique has been used widely in this context.[2] Recently, cluster studies in which the exact Madelung potential has been included in the Hamiltonian[50] or where the correct embedding in the host crystal is taken into account[51–53] have also been reported. However, it is not uncommon to see cluster studies of oxide surfaces in which the long range coulombic interactions are totally neglected. In these studies, the cluster model consists only of a set of atoms without any representation of the Madelung potential of the extended crystal. It is well known that the Madelung potential is a very slowly convergent series, so that the use of truncated clusters without a PC embedding may result in anomalous values of the Madelung field. Nevertheless, there is enough empirical evidence that clusters without any PC embedding give results consistent with the chemical intuition and which are not too different from those obtained with a PC representation of the Madelung potential.[30–38]

In this article, we present for the first time a systematic study of the results given by cluster models of an ionic oxide surface, MgO (100), with and without embedding in PCs. The problems considered involve surface electronic structure, surface reactivity, vibrations of the adsorbed species, etc. We will show that, in general, the inclusion of the long range coulombic interactions guarantees more stable results as a function of the cluster size, but that it is not uncommon that clusters with and without PCs give similar results. We will also attempt a rationalization of this behavior in terms of intrinsic ionic nature of the MgO clusters and of convergence of the Madelung potential versus cluster size.

Computational Details

We have performed all electron Hartree–Fock (HF) calculations on various Mg_nO_n cluster models of the MgO surface. Some clusters are centered around an oxygen atom when the interaction occurs at this site, and we denote these clusters as O_nMg_n; when the interaction occurs at a surface cation the cluster is of the type Mg_nO_n (Fig. 1). The clusters used are stoichiometric and include the same number of Mg and O atoms. The Madelung potential has been taken into account by embedding the clusters in a large array of PCs of nominal values of $+2$ or -2. This is consistent with the largely ionic nature of bulk and surface MgO.[16,28] For the surface models, a $(13 \times 13 \times 4)$ array of PCs has been chosen to simulate the Madelung potential at the adsorption site.[9] The presence of these charges around the cluster induces an artificial polarization of the oxygen atoms at the cluster periphery. Techniques have been developed to remove this artifact;[25,27,54] they are based on the use of effective core potentials (ECP) to represent the finite size of the ions. We have used this technique in one case to compare the behavior of a MgO cluster with and without PCs and with PCs and ECPs.

The reactivity of CO_2 with surface, five-coordinated (O_{5c}) and step, four-coordinated (O_{4c}) oxide

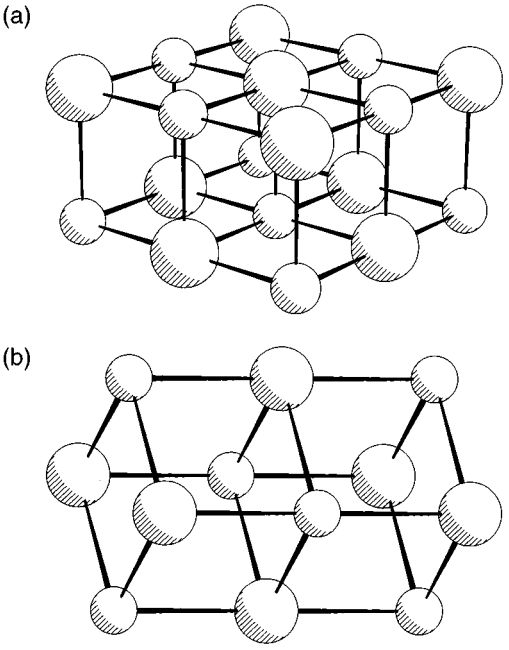

FIGURE 1. (a) O_9Mg_9 cluster model of an O^{2-} site of the MgO (100) surface. Interchange of the first with the second layer gives the Mg_9O_9 cluster used to model a Mg^{2+} site. A O_5Mg_5 cluster can be obtained by cutting the eight corners of the O_9Mg_9 cluster. (b) O_6Mg_6 cluster model of an edge site of the MgO (100) surface. Clusters with and without embedding in point charges have been used.

anions has been modeled by means of O_9Mg_9, O_5Mg_5 (surface) and O_6Mg_6 (step) clusters (Fig. 1). The central Mg^{2+} ion in Mg_nO_n and the five nearest-neighbor Mg^{2+} ions to the central oxygen in O_nMg_n clusters have been treated with a $[13s8p/6s3p]$ basis,[9] which includes a good representation of the Mg $3s$ and $3p$ orbitals; the other Mg^{2+} ions have been treated with a $[12s7p/5s2p]$ basis.[9] In O_9Mg_9, the four Mg^{2+} ions in the second layer were treated with a $[8s4p/2s1p]$ SZ basis set.[55] For the oxygen atoms of MgO we used a $[8s4p/4s2p]$ DZ basis.[55] For CO_2 we used a standard DZP basis set.[56] To better identify the different contributions to the interaction energy for clusters with and without PCs we have performed a constrained space orbital variation (CSOV).[57,58] This technique allows one to measure the relative importance of polarization and charge transfer effects in the bonding of an adsorbate to a surface. Details about this technique and its application to oxide surfaces can be found in refs. 7, 9, 16, and 22. We have also considered the interaction of a neutral H atom and a H^+ proton with the surface oxygen of O_9Mg_9. The basis set for H is of DZP quality;[55] therefore, this basis is of higher quality than the DZ basis used for the MgO clusters, but we do not expect any significant imbalance in the description of the interaction.

As an example of adsorption of a molecule with a permanent dipole moment we chose water interacting with surface cations of MgO. Two cluster models of a surface Mg^{2+} site have been considered, Mg_5O_5 and Mg_9O_9, with and without PCs. Adsorption of CO on surface, five-coordinated Mg_{5c} and on step, four-coordinated Mg_{4c} sites has been studied by means of Mg_5O_5 (surface), Mg_6O_6, and $Mg_{10}O_{10}$ (step) clusters (Fig. 2). In this case we have also performed a full vibrational analysis to determine the CO ω_e by means of finite differences of analytical first derivatives. The Mg and O basis set is the same as that described previously, whereas for C and O a $[9s5p/4s3p]$ basis has been used[59] as in previous studies on this system.[7,9,10]

Finally, we have considered the electronic structure of F_s^+ color centers on the MgO surface. These defects formally correspond to the removal of an O^- ion. Therefore, an F_s^+ center is paramagnetic and the localization of the unpaired electron can be determined by electron spin resonance (ESR) experiments.[60] We have considered $[O_8Mg_9]^+$, $[O_{12}Mg_{13}]^+$, and $[O_{20}Mg_{21}]^+$ models of F_s^+ centers. The same clusters have been used recently for a study of the electronic properties of F_s centers

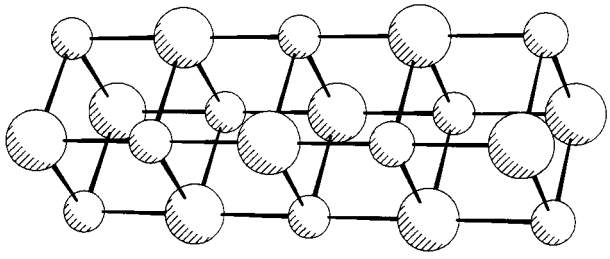

FIGURE 2. The $Mg_{10}O_{10}$ cluster model of a Mg^{2+} cation at an edge site of the MgO (100) surface. A smaller cluster, Mg_6O_6, has been used to model adsorption at the same site. This second cluster has been obtained from $Mg_{10}O_{10}$ by removing the outer eight ions.

and the reader is referred to ref. 61 for details about the basis sets used. Determination of hyperfine coupling constants has been done by performing unrestricted HF calculations; the value of $\langle S^2 \rangle = 0.75$ guarantees that the eigenfunction corresponds to a pure doublet state. The calculations have been performed with the HONDO-8.5 program package[62] on IBM Risc 6000 workstations.

Results and Discussion

ADSORPTION AND REACTIVITY

CO_2 on O^{2-} Sites

A previous study has shown that an O_{5c} site of MgO is very unreactive and that CO_2 does not form a stable surface carbonate at the (100) terraces of the MgO surface.[15] Here we have performed new calculations and we have determined a section of the potential energy surface by optimizing the CO_2 structure for various fixed $O_{5c}—CO_2$ distances. We have considered three models: a bare O_nMg_n cluster; the same cluster embedded in PCs, and in PCs and ECPs ($n = 5, 9$). The potential energy curves for CO_2 on O_9Mg_9 (Fig. 3) are purely repulsive and similar with and without PCs; this seems to indicate a minor effect of the surrounding PCs on the mechanism of interaction. Both curves show a nonmonotone behavior which arises from the energetic balance between the price needed to bend CO_2 and the energy gain due to the formation of the surface carbonate.[22] At a distance of 2.8 bohr from the surface, the geometrical parameters of adsorbed CO_2 are virtually indistinguishable: $r(C—O)$ is 1.202 Å and $\alpha(OCO)$ is 138° for the case with PCs, whereas $r(C—O) = 1.205$

Å and α(OCO) = 137° without. The similar geometry reflects a similar interaction. This is confirmed by the results of the CSOV analysis. The terms contributing to the final interaction energy are similar with and without PCs (Table I). This is particularly significant for the donation and back-donation contributions, but also for the initial Frozen orbital term which accounts for the Pauli repulsion and the electrostatic attraction between the interacting units (Table I). On the other hand, a smaller cluster, O_5Mg_5, gives completely different results with and without PCs. The potential energy curve computed with PCs is very similar to those obtained for O_9Mg_9 and shows the same repulsive behavior (Fig. 3). When CO_2 is adsorbed on bare O_5Mg_5, however, the curve exhibits a deep minimum separated from the dissociation limit by an activation barrier. In this minimum, CO_2 is still unbound with respect to dissociation into neutral fragments, but by 0.2 eV only (Fig. 3). The CSOV analysis (Table I) shows that the different behavior of O_5Mg_5 and O_5Mg_5 + PCs must be ascribed to the different initial repulsion and to the larger charge transfer from MgO to CO_2 occurring when the PCs are not included. This is because the surface O^{2-} ion, unstable in the gas phase, is stabilized by the Madelung potential which, on a small cluster like O_5Mg_5, can be very different from that of the real surface; the consequence is a less stable and more reactive oxide.[22]

This is what happens at MgO step sites. A four-coordinated oxygen is much more reactive than a five-coordinated one because the Madelung potential at these sites is lower than on the regular surface sites.[15] CO_2 forms a stable surface carbonate at the low-coordinated defect sites of the surface without energy barrier.[15] The step site of MgO has been represented by a O_6Mg_6 cluster. The geometry optimization with O_6Mg_6 and O_6Mg_6 + PCs results in not too different geometries but in quite different adsorption energies (Table II). In particular, in the absence of external PCs the interaction is stronger, 2.4 eV versus 1.1 eV (Table II), and the CO_2 molecule is slightly more activated, as shown by a smaller OCO angle and by a longer *r*(CO) (Table II). The CSOV analysis (Table I) helps to understand the origin of the different reactivity. In particular, it shows that the larger stability of

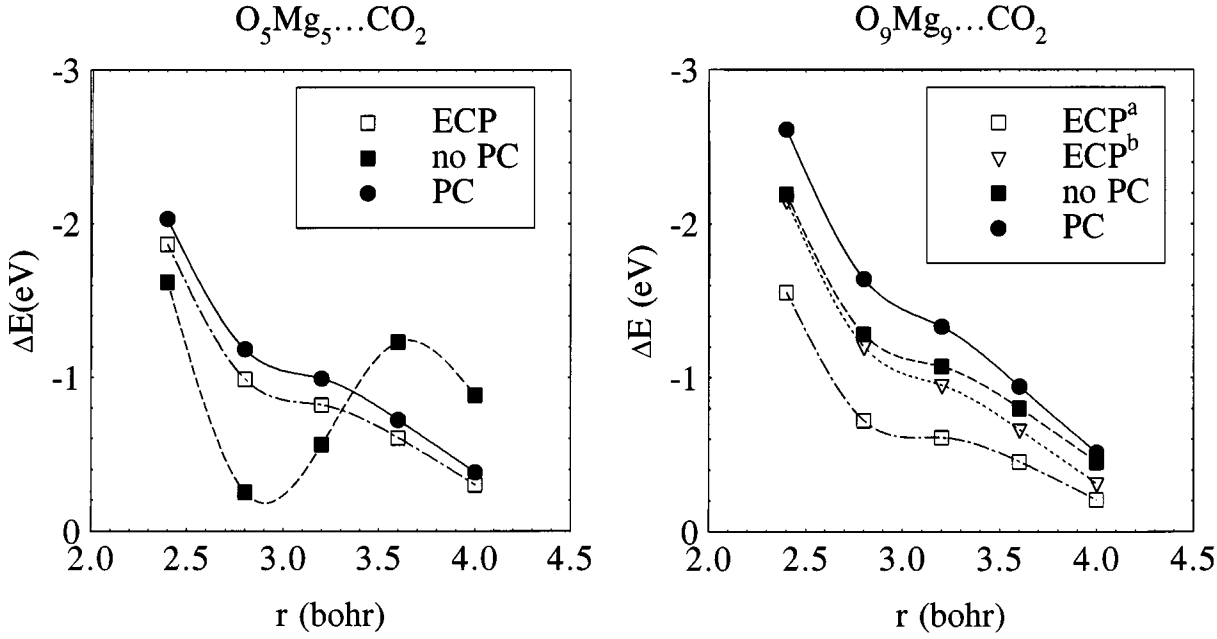

FIGURE 3. Potential energy curves for the interaction of CO_2 with a surface O^{2-} site of MgO. Left: O_5Mg_5; right: O_9Mg_9. For each surface—CO_2 distance the internal geometrical parameters of adsorbed CO_2 have been reoptimized. PC: the cluster is surrounded by a large array of point charges; no PC: the cluster is not surrounded by point charges; ECP: the cluster is surrounded by a large array of point charges and the nearest-neighbor Mg^{2+} ions to the cluster oxygens are described by an effective core potential (ECP). Two cases are reported for O_9Mg_9: ECP^a, each O ion is completely surrounded by ECPs (16 in total); ECP^b: only the O ions in the first layer are surrounded by ECPs (8 in total).

TABLE I.
CSOV Analysis for CO_2 Adsorbed on O_9Mg_9 and O_5Mg_5 (Surface) and O_6Mg_6 (Edge) Cluster Models of the MgO Surface—Clusters with and without Point Charges (PCs) Have Been Considered.[a]

	O_9Mg_9—CO_2				O_5Mg_5—CO_2				O_6Mg_6—CO_2			
	PCs		No PCs		PCs		No PCs		PCs		No PCs	
Cluster	ΔE	$\Delta\mu$	ΔE	$\Delta\mu$	ΔE	$\Delta\mu$	ΔE	$\Delta\mu$	ΔE	$\Delta\mu$	ΔE	$\Delta\mu$
Frozen orbital	−7.20	—	−7.20	—	−6.58	—	−8.32	—	−5.41	—	−5.27	—
MgO polarization	+0.79	−0.11	+0.84	−0.08	+0.61	−0.16	+0.01	−0.11	+0.87	−0.14	+1.06	−0.18
MgO donation	+4.77	−1.11	+4.96	−1.02	+4.88	−1.25	+5.48	−1.52	+5.10	−0.85	+5.54	−1.23
CO_2 polarization	+1.27	+0.03	+1.33	−0.01	+1.23	+0.02	+1.66	−0.03	+1.75	+0.10	+2.04	−0.01
CO_2 donation	+0.29	+0.09	+0.30	+0.07	+0.24	+0.10	+0.38	+0.11	+0.25	+0.16	+0.29	+0.06

[a]Energy change, ΔE, in eV; dipole moment change, $\Delta\mu$, in a.u.

the cluster without PCs is primarily due to the larger donation of charge from the surface to CO_2, in analogy with the O_5Mg_5 case. This is shown not only by the energy gain at the donation step, but also by the large change in the dipole moment, which indicates substantial flow of charge from the oxide anion to the adsorbate. This means that the electrons are less bound to the oxide anion and more easily transferred to an interacting molecule. Again, the role of the Madelung potential is essential. The underestimation of this term leads to a ''too reactive'' oxide, as already shown for the case of O_5Mg_5.

We consider now the effect of using ECPs to represent the finite size of the ions instead of PCs. We used ECPs[63] to represent the next shell of Mg^{2+} ions at the cluster border. This is an approach to the more elaborate *ab initio* model potential of Barandiaran and Seijo.[64] In O_5Mg_5 this means that the 12 + 2 PCs nearest neighbors to the O^{2-} ions have been replaced by ECPs; in the first layer, the central O^{2-} ion is surrounded by real Mg^{2+} cations. In O_9Mg_9, eight additional oxygens are present (Fig. 1) and 16 ECPs have been used to represent the nearest-neighbor Mg^{2+} ions to the peripheral oxygens. In these models, each O ion is thus completely surrounded by either real Mg ions or ECPs. To show how the use of ECPs reduces the artificial polarization of the O ions by the PCs, we consider also a cluster in which only the surface oxygens are embedded in 8 ECPs, whereas the second layer oxygens are surrounded by PCs. The results for CO_2 adsorption are graphically represented in Figure 3. On O_5Mg_5 the effect of the ECPs is rather small and the curves obtained with PCs or with PCs and ECPs are similar. This is not the case of O_9Mg_9, in which the curve obtained with the 16 ECPs is considerably different and, in particular, is less repulsive, than with PCs. The reason for the different response of the two clusters is that, in the first case, O_5Mg_5, there are no O ions at the cluster border in the first layer but only in the second; the addition of the ECPs changes the polarization of these second layer oxygens but does not affect in a marked way the reactivity of the central surface oxygen. In O_9Mg_9, on the other hand, there are four surface O ions at the cluster border which are artificially polarized by the neighboring charges, an artifact removed by the ECPs. This polarization is large enough to change the electrostatic potential and the charge density around the central oxygen, leading to a different reactivity. The polarization of the second-layer oxygens, however, is nonnegligible. This is shown by the model in which only 8 ECPs in the cluster first layer have been included. The corresponding curve (see ECP^b in Fig. 3) is between that of O_9Mg_9 + PCs and O_9Mg_9 + PCs + 16 ECP. These results show the importance of removing the artificial polarization of the border oxygens induced by the PCs. The use of ECPs is an efficient way to eliminate or reduce this problem. It should be noted that the use of ECPs to replace the −2 charges is much less important. In fact, the polarizability of the Mg^{2+} cations is extremely low, and does not change appreciably when the neighboring ions are described by simple −2 PCs or by PCs and ECPs.

It is possible to conclude that O_9Mg_9 is probably the smallest cluster that can be used to model adsorption on an oxide anion of MgO. This is also due to the fact that the cluster is built of two layers which are almost neutral, at variance with the O_5Mg_5 cluster in which each layer contains four cations and one anion (or vice versa).

TABLE II.
Equilibrium Properties of CO_2, H_2O, and CO Adsorbed on O^{2-} or Mg^{2+} Ions of MgO Surface.

System and properties	PCs	No PCs
O_6Mg_6—CO_2 (edge site)		
z_e (O—CO_2) (Å)	1.41	1.37
r_e (C—O) (Å)	1.22	1.24
α(OCO) (degrees)	137	134
D_e (eV)	1.13	2.42
Mg_5O_5—H_2O (surface)		
z_e (Mg—OH_2) (Å)	2.14	2.10
r_e (O—H) (Å)	0.94	0.94
α(HOH) (degrees)	110	112
D_e (eV)	0.64	4.12
Mg_9O_9—H_2O (surface)		
z_e (Mg—OH_2) (Å)	2.17	2.25
r_e (O—H) (Å)	0.94	0.94
α(HOH) (degrees)	110	110
D_e (eV)	0.62	0.26
Mg_5O_5—CO (surface)		
z_e (Mg—CO) (Å)	2.48	unbound
Δz (Mg^{2+})[a] (Å)	0.05	−0.33
D_e (eV)	0.24	unbound
Mg_6O_6—CO (edge)		
z_e (Mg—CO) (Å)	2.41	2.45
Δz (Mg^{2+}) (Å)	0.03	0.02
$\Delta\omega_e$ (C—O)[b] (cm^{-1})	40	20
D_e (eV)	0.38	0.33
$Mg_{10}O_{10}$—CO (edge)		
z_e (Mg—C) (Å)	2.45	2.45
Δz (Mg^{2+}) (Å)	0.03	−0.02
$\Delta\omega_e$ (C—O)[b] (cm^{-1})	48	31
D_e (eV)	0.34	0.30

[a] Vertical relaxation of the surface Mg^{2+} ions (surface rumpling).
[b] Experimental $\Delta\omega_e$ (C—O) = 21 cm^{-1}; ref. 67.

H and H^+ on O^{2-} Sites

We have seen that the O_9Mg_9 cluster shows virtually the same reactivity toward CO_2 independently of the inclusion of the Madelung potential. To confirm this result we have considered the interaction of this cluster with a neutral H atom and with a proton. The potential energy curve for the interaction with neutral H is repulsive, and further shows the very low reactivity of a surface oxygen of MgO when the Madelung term is properly described. The two curves for O_9Mg_9 and O_9Mg_9 + PCs are very similar (Fig. 4). Conditions are different for the interaction with a proton (Fig. 5). Here there is a strong and attractive electrostatic interaction. The interaction energy can be divided into the sum of three contributions: the interaction of a +1 charge with the surface electrostatic potential; the polarization of the surface in response to the presence of the charge; and the charge transfer from the surface oxygen to the empty orbitals of the proton (Table III). These contributions can be distinguished by computing a cluster with a +1 PC and a cluster with a real H^+ ion. The interaction energy curve for H^+ on O_9Mg_9 is much deeper than for O_9Mg_9 + PCs (Fig. 5). This is because the electrostatic potential in the two cases is different[65]; in particular, without PCs, the EP is smaller. The other two terms, the cluster polarization and the charge transfer, are almost identical with and without PCs (Table III). We have repeated the calculation with O_5Mg_5 and O_5Mg_5 + PCs and we found a reversed behavior: the interaction of the proton is stronger for the case with PCs. The reason is primarily the different value of the electrostatic potential in O_9Mg_9 and O_5Mg_5, although there are also differences in the cluster polarization (see Table III). In the absence of surrounding PCs, the electrostatic potential oscillates strongly as a function of the number of cations or anions on the cluster surface (or, in

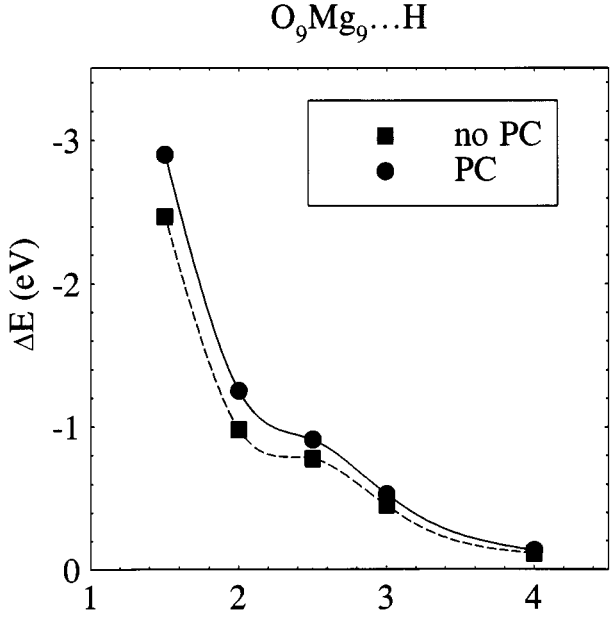

FIGURE 4. Potential energy curve for the interaction of a neutral H atom with a surface O^{2-} site of O_9Mg_9.

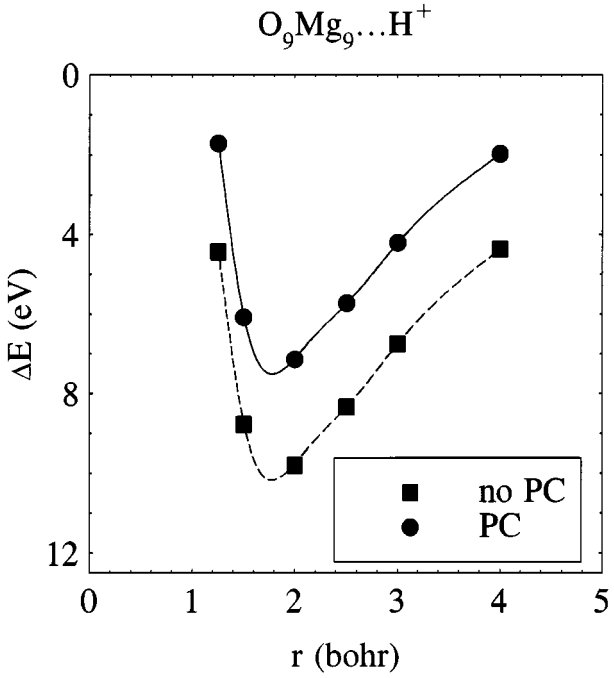

FIGURE 5. Potential energy curve for the interaction of a proton with a surface O^{2-} site of O_9Mg_9.

other words, of the cluster size).[65] Therefore, an important conclusion is that even when the use of clusters without representation of the long range coulombic potential is acceptable for the adsorption of neutral molecules, these models should be used with great care to study the interaction of charged species or in general for cases in which electrostatic effects play a dominant role.

H_2O on Mg^{2+} Sites

We have studied the nondissociative adsorption of water as an example of interaction of the MgO surface with a molecule with permanent dipole moment. We have considered the perpendicular approach of the molecule on top of a Mg^{2+} cation. Recent studies have shown that there are several possible adsorption modes for this molecule,[47,48] but our purpose is to compare clusters of different size with and without PC embedding. The clusters considered are Mg_5O_5 and Mg_9O_9. The substrate atoms have been kept fixed and a full geometry optimization has been performed for the adsorbed H_2O molecule (Table II). The geometry of the adsorbate is practically independent of the cluster model used; the largest variations occur for the $Mg—OH_2$ distance which goes from 2.10 Å on Mg_5O_5 to 2.25 Å on Mg_9O_9; the clusters with PCs are 2.14 and 2.17 Å, respectively (Table II). The internal H_2O geometrical parameters are virtually the same for all models considered. Conditions are quite different when one considers adsorption energy. The two clusters embedded in PCs give the same adsorption energy, $\approx$ 0.6 eV; on bare Mg_9O_9, the D_e is reduced to 0.26 eV (Table II). On bare Mg_5O_5, however, the computed D_e is 4.1 eV! This is a strong deviation from the other results, which is indicative of a completely different electrostatic potential (EP) in the chemisorption region for this latter cluster. The small geometrical distortions of adsorbed versus free water molecule suggest a highly electrostatic interaction with the surface. We have computed the EP along the normal to the Mg^{2+} adsorption site for the four models and we indeed found a totally different EP for Mg_5O_5 without PCs. In particular, the EP values computed at 4 bohr from the surface, close to the equilibrium position of the water molecule, are: Mg_9O_9 + PCs = 1.98 eV; Mg_5O_5 + PCs = 1.82 eV; Mg_9O_9 = 1.51 eV; and Mg_5O_5 = −2.17 eV. We notice that the EP values for the two clusters embedded in PCs are similar, consistent with the similarly computed D_e values. For bare Mg_9O_9, the EP is smaller but has the same sign of the clusters with PCs; for Mg_5O_5, on the other hand, even the sign of the EP is reversed, indicating that this cluster is not well suited for the calculation of adsorption energies of electrostatically bound molecules.

TABLE III.
Energy Contributions (eV) to Interaction of Proton with Surface O^{2-} Ion of MgO (100) Surface.

	O_5Mg_5		O_9Mg_9	
Cluster	PCs	No PCs	PCs	No PCs
(a) Electrostatic interaction	2.31	0.73	1.39	3.89
(b) Surface polarization	1.70	2.93	2.09	2.23
(c) Charge transfer	3.82	3.46	3.67	3.68
Sum (a) + (b) + (c)	7.83	7.12	7.15	9.80

CO on Mg^{2+} Sites

Adsorption of CO on MgO is another example of interaction with surfaces dominated by electrostatics.[7,9] The determination of the binding energy of CO on MgO is a delicate problem, which has been the subject of a number of theoretical investigations.[7,13,14,18,25,27,28] Here we do not address this point specifically, but rather compare clusters with PC embedding with bare MgO clusters. To this end we have optimized the geometry of a CO molecule vertically adsorbed on a Mg^{2+} cation of the MgO surface; the substrate is represented by the Mg_5O_5 cluster. In contrast to the previous case, here the surface cation where CO is adsorbed was allowed to relax in the optimization while all the other atoms of the cluster were fixed at the lattice positions of bulk MgO. The same process has been considered for a step site, and the cluster used is Mg_6O_6 (Fig. 1). The response of the two approaches, with and without PCs, is quite different for the surface site. First, virtually no surface rumpling is found with Mg_5O_5 + PCs, in agreement with experiment,[66] whereas substantial relaxation of the position of the Mg^{2+} ion is found with Mg_5O_5 [see $\Delta z(Mg^{2+})$ in Table II]. Second, while CO is bound on Mg_5O_5 + PCs by 0.23 eV (not corrected by the BSSE), no binding at all is found between CO and Mg_5O_5 without PCs. This is a qualitatively significant difference as it is experimentally established that CO is weakly bound at MgO terraces (see, e.g., ref. 1 and references therein). In this respect, the use of a cluster without inclusion of long-range electrostatic terms leads to qualitatively incorrect results, as already found for the case involving water.

This is not the case for the edge site. In fact, CO is adsorbed at a Mg_{4c} cation with practically the same binding energy, 0.3 eV, and the same geometry, irrespective of the presence of the external PCs or the cluster size (see Table II). With a more exposed cation, the EP is dominated by the local contribution from the ions around the adsorption site and the effect of the distant ions (or PCs) is less important. This may explain the different response of clusters of similar size (Mg_5O_5 or Mg_6O_6) in the description of the adsorption at different sites like a surface or a step cation.

VIBRATIONAL FREQUENCIES: CO ON MgO

In a recent article, Pelmenschikov et al.[38] suggested that molecular models of ionic materials without embedding accurately reproduce the vibrational shifts of adsorbed molecules. For CO adsorbed on MgO, ω shifts of 10, 21, and 60 cm^{-1} with respect to the free molecule have been measured and assigned to CO adsorbed on five-, four-, and three-coordinated Mg^{2+} cations (surface, step, and corner sites, respectively).[67] In ref. 38, it has been shown that the ω shifts of CO adsorbed on step and corner sites are quantitatively reproduced by using HF wave functions and small MgO clusters without any representation of the Madelung potential. No attempt has been done, however, to evaluate the importance of the Madelung term in determining the CO vibrational frequency. Thus, we compare the adsorption of CO on Mg_6O_6, Mg_6O_6 + PCs, $Mg_{10}O_{10}$, and $Mg_{10}O_{10}$ + PCs cluster models of an edge site (Fig. 2). The use of two clusters of different size will provide some information about the converge of the results with cluster size. No comparison is possible for the surface site because, as mentioned above, no minimum is found for CO adsorbed on Mg_5O_5 without PCs.

We consider first the smallest model. The CO ω shift computed with Mg_6O_6 + PCs is of $+40$ cm^{-1}; the shift computed with Mg_6O_6 is $+20$ cm^{-1}. Both shifts are in the right direction (the CO ω_e is higher than in the gas phase). The value obtained without PCs is in excellent agreement with the experimental data, $+21$ cm^{-1},[67] and with the results of ref. 38. The obvious conclusion would be that the presence of the PCs results in a too-large ω shift.[38] This is certainly true at the HF level of theory but the question of the importance of correlation effects remains open. The ω shift of CO adsorbed on MgO has a largely electrostatic origin.[7,9] In particular, it is due to a combination of the wall effect, a term arising from the Pauli repulsion due to the stretching of the molecule against the rigid surface,[7] and a term due to the interaction between the surface electric field and the CO dynamic dipole moment, $d\mu/dr$.[9] This second term dominates when CO is adsorbed on free or exposed cations.[9,10] One important contribution to the CO ω shift is therefore the CO dynamic dipole moment, which in HF is much larger than the experimental value of -0.6 a.u. (it is -1.0 a.u. with the present basis set)[9]; CASSCF calculations where the active space consists of the 1π, 5σ, $2\pi^*$, and $6\sigma^*$ orbitals give $d\mu/dr = -0.7$, much closer to the experimental value. Thus, correlation effects reduce the value of the CO dynamic dipole moment and may affect the value of the CO ω shift. In fact, for uniform electric fields the field-induced

CO ω shift is a function of both the slope and the curvature of the dipole moment curve.[68,69]

We have computed the vibrational frequency of the CO molecule in the presence of uniform fields, $F = 0.01$ a.u. and $F = 0.05$ a.u., and of a distribution of PCs simulating the edge site of MgO; in practice, we replaced the ions of the Mg_6O_6 + PCs cluster by ± 2 PCs. The CO ω_e has been determined for both SCF and CASSCF wave functions and compared with that of free CO. For a field $F = 0.01$ a.u. the CO ω shift is virtually the same, $+23$ cm^{-1} in SCF, and $+22$ cm^{-1} in CASSCF. For a larger field, $F = 0.05$ a.u., the shift at the SCF level, $+112$ cm^{-1}, is much larger than in CASSCF, $+69$ cm^{-1}. For the nonhomogeneous field given by the PCs simulating the edge site we again found a similar shift in SCF, $+38$ cm^{-1}, and CASSCF, $+33$ cm^{-1}. These results indicate that, for small electric fields, the CO ω shifts computed at correlated and uncorrelated levels are similar, but for larger fields correlation effects lower $\Delta\omega$ substantially. This is the case, for instance, of CO adsorbed at corner sites where the shift of 60 cm^{-1} is largely due to the field–dipole interaction.[10] An additional warning in computing small shifts of the order of a few cm^{-1} is that the BSSE can affect these quantities as well as the adsorption energies. A proper consideration of this error may also be necessary when discussing accuracies within 2–3 cm^{-1}. Of course, the use of clusters with surrounding PCs to determine vibrational shifts is not free from limitations; in fact, as already mentioned, the PCs induce an artificial polarization of the oxygen atoms at the cluster border with change of the cluster electric field and of the Pauli repulsion with the adsorbed molecule. These effects, however, can be reduced by placing, at the PCs positions, ECPs or projector operators that account for the finite size of the ions.[25,27]

Another important point to investigate is the cluster size dependence of the results. We have considered a larger cluster, $Mg_{10}O_{10}$, and repeated the geometry optimization and vibrational analysis as for the Mg_6O_6 case. The results (Table II) clearly show that the adsorbate geometry and binding energy are relatively well converged for both models with and without PCs and that similar values are found for the two clusters within our error limits. On the other hand, the CO vibrational shift is 8 cm^{-1} (PC) and 11 cm^{-1} (no PC) higher in the larger cluster (Table II) compared with the smaller one. While this is a small change in absolute value, it is relevant when the total shift is of the order of 20–30 cm^{-1} as in the present case. In conclusion, the computed shifts can be considered accurate with error limits of ± 10 cm^{-1}, but a more precise determination of this property may require considerably more refined models and theoretical methods.

SURFACE ELECTRONIC PROPERTIES

As a last example of the importance of the inclusion of the Madelung potential we consider the case of paramagnetic F_s^+ centers on the surface of MgO. These centers are quite important in several adsorption processes because they exhibit a much higher reactivity than that of the regular surface.[71] Furthermore, their electronic structure can be characterized by means of ESR techniques and the calculation of observable properties like the hyperfine coupling constants, **A**, represents an important test of the adequacy of the model used. Recent studies have shown that, on the electronic ground state, the unpaired electron is entirely localized in the vacancy, and that this is consistent with a small value of **A**.[60] **A** is the hyperfine coupling constant of the electronic spin with the nuclear spin of the ^{25}Mg nucleus; we have determined the isotropic part of **A**, a_{iso} (the Fermi contact term), which is about 10 G in absolute value according to experiment (see ref. 60 and references therein). We have considered clusters of different sizes, $[O_8Mg_9]^+$, $[O_{12}Mg_{13}]^+$, and $[O_{20}Mg_{21}]^+$; as usual, the clusters have been computed with and without surrounding PCs. The a_{iso} values are reported for the four equivalent Mg ions in the first layer and for the single Mg ion in the second layer (Table IV). When the largest cluster is considered, $[O_{20}Mg_{21}]^+$, the results with and without PCs are similar (Table IV). The small a_{iso} values, about 4–5 G, are consistent with the un-

TABLE IV.
Hyperfine Coupling Constants, a_{iso}, for Paramagnetic F_s^+ Centers on MgO Surface.

Cluster	a_{iso} (G) Mg first layer	a_{iso} (G) Mg second layer
$[O_8Mg_9]^+$ + PCs	−6.0	−5.2
$[O_{12}Mg_{13}]^+$ + PCs	−5.5	−3.5
$[O_{20}Mg_{21}]^+$ + PCs	−4.2	−5.2
$[O_8Mg_9]^+$	0.0	−5.7
$[O_{12}Mg_{13}]^+$	3.5	−44.9
$[O_{20}Mg_{21}]^+$	−4.7	−1.1
Experimental (ref. 60)	$\approx -8/-10$	≈ -12

paired electron being localized in the vacancy and not on the 3*s* levels of the Mg ions. The use of smaller clusters embedded in PCs gives essentially the same result (see Table IV). Small variations are found in the a_{iso} values as a function of the cluster size, but these oscillations are never larger than 1−2 G, clearly indicating the same electronic structure for all clusters (Table IV). On the contrary, dramatic changes occur when clusters without embedding are considered. In $[O_{12}Mg_{13}]^+$, a large a_{iso} of -45 G is found for the Mg ion in the second layer, indicating a strong localization of the unpaired electron on this atom. This is different from the other clusters and in contradiction with the experiment. The even smaller $[O_8Mg_9]^+$ cluster, on the other hand, gives no spin density at all on the Mg ions in the first layer (a_{iso} is zero, Table IV) and a small spin density on Mg^{2+} in the second layer. Again, this contradicts the experimental observation.

Clearly, the absence of the long range potential leads to dramatic changes in the electronic structure and in strong oscillations as function of the cluster size. This is not surprising if we think that the Madelung term is a slowly convergent series. The fact that some clusters exhibit similar behavior with and without PCs simply indicates a fortuitously similar value of the truncated summation with the infinite one.

Conclusions

In this study, we have considered the electronic properties and the reactivity of MgO clusters with and without a PC representation of the Madelung potential of the extended surface. Depending on the size of the clusters considered, different results are obtained. In fact, for some clusters we found a similar behavior with and without the surrounding PCs. This is the case of adsorption of H and CO_2 on the O_9Mg_9 cluster model of a surface oxygen, of the Mg_6O_6 and $Mg_{10}O_{10}$ models of adsorption of CO at a step Mg^{2+} site, and of the $[O_{20}Mg_{21}]^+$ cluster used to describe the F_s^+ centers. For all these clusters, the results seem to be virtually independent of the presence of the PCs. On the other hand, we have found a considerable number of cases in which clusters without embedding in PCs give results completely different than those with PCs and, more importantly, which are in contrast to the experimental evidence. This is the case for smaller cluster models, like O_5Mg_5 and Mg_5O_5, or of the $[O_{12}Mg_{13}]^+$ and $[O_8Mg_9]^+$ models of surface F_s^+ centers. This suggests that inclusion of the long range coulombic interactions is essential when the clusters are small.

The reactivity and the electronic structure of oxide surfaces is largely a function of the Madelung potential at a given site. Therefore, several electronic and chemical properties of ionic materials can be explained simply in terms of electrostatics. For instance, the trends in core level binding energies of oxygen anions[72] and metal cations[73] in alkaline-earth oxides can be easily rationalized in terms of the Madelung potential at the site where the photoionization occurs. Also, the basicity of oxide surfaces is a chemical property directly connected to the Madelung potential and not, as often assumed, to the net charge of an ion.[22] In particular, a larger Madelung potential results in a more stable and less basic anion (e.g., the surface sites of MgO) while a lower Madelung potential leads to a stronger donor ability (e.g., the edges and corner sites of the surface). In this way, it is also possible to understand the increasing basic character in the series MgO, CaO, SrO, and BaO.[22]

From the previous discussion it is apparent that the Madelung potential is a crucial quantity in determining the properties of an ionic material. Cluster models of an ionic oxide must correctly describe this contribution and the use of embedding in PCs is a simple, yet efficient, way to do this. It has been suggested that in MgO values of PCs lower than ± 2 give results in better agreement with the experiment.[13,24] The use of PCs is less obvious for materials in which the bonding has a mixed ionic-covalent character, like in SiO_2 or TiO_2. It is possible that clusters without representation of the Madelung field give similar results. In fact, the charge separation determining the ionic character of the material develops very rapidly within a cluster, even when the size is relatively small. This means that an ''internal'' Madelung stabilization develops with the growth of the cluster. For instance, we have recently found that a Ti_7O_{14} cluster model of TiO_2 (110)[74] and a $Cu_{28}O_{14}$ model of Cu_2O (111)[75] surfaces, respectively, give similar results for the adsorption of CO on cation sites with and without embedding in PCs. However, there is no guarantee that for a ''small'' cluster the Madelung potential at a given site resembles that of the real surface. Thus, for not completely ionic systems, where one may wonder which is the exact Madelung field, it is desirable to compute the properties of interest as a function of the field. Usually, slight to rather large variations

(up to 50%) on the Madelung field do not result in large variations of the properties.[76]

In conclusion, we have shown that the use of an external field helps in stabilizing the Madelung potential within cluster models of ionic materials and strongly reduces the oscillations connected with the cluster size.

Acknowledgments

This work has been supported by the Italian Ministry of University and Research, and CICyt Project PB92-0766-CO2-01 and PB95-1247 of the Spanish Ministerio de Education y Ciencia. A. M. F. thanks the Computational Center of Catalunya (CESCA) for the financial support for her stay at the University of Barcelona through the Human Capital and Mobility Programme. We are grateful to NATO for Collaborative Research Grant No. 941191.

References

1. J. Sauer, P. Ugliengo, E. Garrone, and V. R. Saunders, *Chem. Rev.*, **94**, 2095 (1994).
2. J. Sauer, *Chem. Rev.*, **89**, 199 (1989).
3. E. A. Colbourn, *Surf. Sci. Rep.*, **15**, 281 (1992).
4. G. Pacchioni, P. S. Bagus, and F. Parmigiani, Eds., *Cluster Models for Surface and Bulk Phenomena* (*NATO ASI Series B, Vol. 283*), Plenum, New York, 1992.
5. E. A. Colbourn and W. C. Mackrodt, *Surf. Sci.*, **143**, 391 (1984).
6. R. Huzimura, Y. Yanagisawa, K. Matsumura, and S. Yamabe, *Phys. Rev. B*, **41**, 3786 (1990).
7. G. Pacchioni, G. Cogliandro, and P. S. Bagus, *Surf. Sci.*, **255**, 344 (1991).
8. K. J. Borve and L. G. M. Pettersson, *J. Phys. Chem.*, **95**, 7401 (1991).
9. G. Pacchioni, G. Cogliandro, and P. S. Bagus, *Int. J. Quant. Chem.*, **42**, 1115 (1992).
10. G. Pacchioni, T. Minerva, and P. S. Bagus, *Surf. Sci.*, **275**, 450 (1992).
11. K. J. Borve, *J. Chem. Phys.*, **96**, 6281 (1992).
12. D. Strömberg, *Surf. Sci.*, **275**, 473 (1992).
13. K. M. Neyman and N. Rösch, *Chem. Phys.*, **168**, 267 (1992).
14. M. Pölchen and V. Staemmler, *J. Chem. Phys.*, **97**, 2583 (1992).
15. G. Pacchioni, *Surf. Sci.*, **281**, 207 (1993).
16. G. Pacchioni, C. Sousa, F. Illas, P. S. Bagus, and F. Parmigiani, *Phys. Rev. B*, **48**, 11573 (1993).
17. K. M. Neyman and N. Rösch, *Surf. Sci.*, **297**, 223 (1993).
18. K. M. Neyman and N. Rösch, *Chem. Phys.*, **177** (1993).
19. A. Freitag, V. Staemmler, D. Cappus, C. A. Ventrice, K. A. Shamery, H. Kuhlenbeck, and H. J. Freund, *Chem. Phys. Lett.*, **210**, 10 (1993).
20. G. Pacchioni and P. S. Bagus, *Phys. Rev. B*, **50**, 2576 (1994).
21. G. Pacchioni, J. M. Ricart, and A. Clotet, *Surf. Sci.*, **315**, 337 (1994).
22. G. Pacchioni, J. M. Ricart, and F. Illas, *J. Am. Chem. Soc.*, **116**, 10152 (1994).
23. A. Snis, I. Panas, and D. Strömberg, *Surf. Sci.*, **310**, L579 (1994).
24. M. Nygren and L. G. M. Pettersson, *Chem. Phys. Lett.*, **230**, 456 (1994).
25. M. Nygren, L. G. M. Pettersson, Z. Barandiaran, and L. Seijo, *J. Chem. Phys.*, **100**, 2010 (1994).
26. H. Nakatsuji, M. Yoshimoto, M. Hada, K. Domen, and C. Hirose, *Surf. Sci.*, **336**, 232 (1995).
27. J. A. Mejias, A. M. Marquez, J. Fernandez-Sanz, M. Fernandez-Garcia, J. M. Ricart, C. Sousa, and F. Illas, *Surf. Sci.*, **327**, 59 (1995).
28. C. Sousa, J. A. Mejias, G. Pacchioni, and F. Illas, *Chem. Phys. Lett.*, **249**, 123 (1996).
29. K. M. Neyman, S. P. Ruzankin, and N. Rösch, *Chem. Phys. Lett.*, **246**, 546 (1995).
30. T. Ito, T. Tashiro, M. Kawasaki, T. Watanabe, K. Toi, and H. Kobayashi, *J. Phys. Chem.*, **95**, 4476 (1991).
31. K. Sawabe, N. Koga, K. Morokuma, and Y. Iwasawa, *J. Chem. Phys.*, **97**, 6871 (1992).
32. K. Sawabe, N. Koga, K. Morokuma, and Y. Iwasawa, *J. Chem. Phys.*, **101**, 4819 (1994).
33. K. Sawabe, K. Morokuma, and Y. Iwasawa, *J. Chem. Phys.*, **101**, 7095 (1994).
34. J. L. Anchell and E. D. Glendening, *J. Phys. Chem.*, **98**, 11582 (1994).
35. Y. Yanagisawa, K. Takaoka, and S. Yamabe, *J. Chem. Soc. Faraday Trans.*, **90**, 2561 (1994).
36. H. Kobayashi, D. R. Salahub, and T. Ito, *J. Phys. Chem.*, **98**, 5487 (1994).
37. Y. Yanagisawa, K. Takaoka, S. Yamabe, and T. Ito, *J. Phys. Chem.*, **99**, 3704 (1995).
38. A. G. Pelmenschikov, G. Morosi, A. Gamba, and S. Coluccia, *J. Phys. Chem.*, **99**, 15018 (1995).
39. M. Causà, R. Dovesi, C. Pisani, and C. Roetti, *Surf. Sci.*, **175**, 551 (1986).
40. R. Dovesi, R. Orlando, F. Ricca, and C. Roetti, *Surf. Sci.*, **186**, 267 (1987).
41. C. A. Scamehorn, A. C. Hess, and M. I. McCarthy, *J. Chem. Phys.*, **99**, 2786 (1993).
42. U. Birkenheuer, J. C. Boettger, and N. Rösch, *J. Chem. Phys.*, **100**, 6826 (1994).
43. W. Langel and M. Parrinello, *Phys. Rev. Lett.*, **73**, 504 (1994).
44. J. Goniakowski and C. Noguera, *Surf. Sci.*, **330**, 337 (1995).
45. R. Nada, A. C. Hess, and C. Pisani, *Surf. Sci.*, **336**, 353 (1995).
46. Y. Ferro, A. Allouche, F. Corà, C. Pisani, and C. Girardet, *Surf. Sci.*, **325**, 139 (1995).
47. M. D. Towler, N. M. Harrison, and M. I. McCarthy, *Phys. Rev. B*, **52**, 5375 (1995).
48. K. Refson, R. A. Wogelius, D. G. Fraser, M. C. Payne, M. H. Lee, and V. Milman, *Phys. Rev. B*, **52**, 10823 (1995).
49. W. Langel and M. Parrinello, *J. Chem. Phys.*, **103**, 3240 (1995).

50. M. A. Nygren, L. G. M. Pettersson, A. Freitag, V. Staemmler, D. H. Gay, and A. L. Rohl, *J. Phys. Chem.*, **100**, 294 (1996).
51. C. Pisani, R. Orlando, and R. Nada, in *Cluster Models for Surface and Bulk Phenomena* (*NATO ASI Series B, Vol. 283*), G. Pacchioni, P. S. Bagus, and F. Parmigiani, Eds., Plenum, New York, 1992, p. 515.
52. C. Pisani, F. Corà, R. Dovesi, and R. Orlando, *J. Electron Spectrosc. Relat. Phenom.*, **96**, 1 (1994).
53. A. Allouche, F. Corà, and C. Girardet, *Chem. Phys.*, **201**, 59 (1995).
54. V. Luana and L. Puejo, *Phys. Rev. B*, **41**, 3800 (1990).
55. S. Huzinaga, Ed., *Gaussian Basis Sets for Molecular Calculations* (*Physical Science Data, Vol. 16*), Elsevier, Amsterdam, 1984.
56. T. H. Dunning and P. J. Hay, *Modern Theoretical Chemistry*, Plenum, New York, 1976.
57. P. S. Bagus, K. Hermann, and C. W. Bauschlicher, *J. Chem. Phys.*, **80**, 4378 (1984).
58. P. S. Bagus and F. Illas, *J. Chem. Phys.*, **96**, 8962 (1992).
59. F. J. van Duijenevled, *IBM Res. Rep. No. RJ 945*, 1971.
60. D. Murphy and E. Giamello, *J. Phys. Chem.*, **99**, 15172 (1995), and references therein.
61. A. M. Ferrari and G. Pacchioni, *J. Phys. Chem.*, **99**, 17010 (1995).
62. M. Dupuis, F. Johnston, and A. Marquez, *HONDO 8.5 for CHEM-Station*, IBM Co., Kingston, NY, 1994.
63. W. J. Stevens, H. Basch, and M. Krauss, *J. Chem. Phys.*, **81**, 6026 (1984).
64. Z. Barandiaran and L. Seijo, *J. Chem. Phys.*, **89**, 5739 (1988).
65. A. M. Ferrari and G. Pacchioni, *Int. J. Quant. Chem.*, **58**, 241 (1996).
66. V. E. Heinrich and P. Cox, *The Surface Science of Meal Oxides*, Cambridge University Press, Cambridge, 1994.
67. L. Marchese, S. Coluccia, G. Martra, and A. Zecchina, *Surf. Sci.*, **269/270**, 135 (1992).
68. D. K. Lambert, *J. Chem. Phys.*, **89**, 3847 (1988).
69. P. S. Bagus, C. J. Nelin, W. Muller, M. R. Philpott, and H. Seki, *Phys. Rev. Lett.*, **58**, 559 (1987).
70. G. Pacchioni, K. Neyman, and N. Rösch, *J. Electron Spectrosc. Relat. Phenom.*, **69**, 13 (1994).
71. A. M. Ferrari and G. Pacchioni, *J. Phys. Chem.*, **100**, 9032 (1996).
72. G. Pacchioni and P. S. Bagus, *Phys. Rev. B*, **50**, 2576 (1994).
73. P. S. Bagus, G. Pacchioni, C. Sousa, T. Minerva, and F. Parmigiani, *Chem. Phys. Lett.*, **196**, 641 (1992).
74. G. Pacchioni, A. M. Ferrari, and P. S. Bagus, *Surf. Sci.*, **350**, 159 (1996), *Surf. Sci.*, to appear.
75. T. Bredow and G. Pacchioni, *Surf. Sci.*, to appear.
76. C. Sousa, F. Illas, and G. Pacchioni, *J. Chem. Phys.*, **99**, 6818 (1993).